Research Square

Preprints are preliminary reports that have not undergone peer review.
They should not be considered conclusive, used to inform clinical practice,
or referenced by the media as validated information.

Dosimetric and radiobiological benefits of FLASH radiotherapy in breast cancer: complementary dose-dependent sparing driven by hypofractionation and FLASH effect

Guoqiang Zhao
Sichuan Cancer Hospital & Institute, Sichuan Cancer Center, Affiliated Cancer Hospital of University of Electronic Science and Technology of China

Junxiang Wu
Sichuan Cancer Hospital & Institute, Sichuan Cancer Center, Affiliated Cancer Hospital of University of Electronic Science and Technology of China

Da Zhang
Sichuan Cancer Hospital & Institute, Sichuan Cancer Center, Affiliated Cancer Hospital of University of Electronic Science and Technology of China

Jie Li
Sichuan Cancer Hospital & Institute, Sichuan Cancer Center, Affiliated Cancer Hospital of University of Electronic Science and Technology of China

Yi Peng
Sichuan Cancer Hospital & Institute, Sichuan Cancer Center, Affiliated Cancer Hospital of University of Electronic Science and Technology of China

Tiziana Malatesta
Isola Tiberina – Gemelli Isola Hospital

Lintao Li
Sichuan Cancer Hospital & Institute, Sichuan Cancer Center, Affiliated Cancer Hospital of University of Electronic Science and Technology of China

Shun Lu
Sichuan Cancer Hospital & Institute, Sichuan Cancer Center, Affiliated Cancer Hospital of University of Electronic Science and Technology of China

Jinyi Lang
Sichuan Cancer Hospital & Institute, Sichuan Cancer Center, Affiliated Cancer Hospital of University of Electronic Science and Technology of China

Xianliang Wang
Sichuan Cancer Hospital & Institute, Sichuan Cancer Center, Affiliated Cancer Hospital of University of Electronic Science and Technology of China

Hao Guo

guohao@scszlyy.org.cn

Sichuan Cancer Hospital & Institute, Sichuan Cancer Center, Affiliated Cancer Hospital of University of Electronic Science and Technology of China

---

Research Article

Keywords: FLASH radiotherapy, Breast cancer; Hypofractionation, Late normal-tissue toxicity

Posted Date: November 18th, 2026

DOI: https://doi.org/10.21203/rs.3.rs-11177787/v1

License: This work is licensed under a Creative Commons Attribution 4.0 International License. Read Full License

Additional Declarations: No competing interests reported.

Dosimetric and radiobiological benefits of FLASH radiotherapy in breast cancer: complementary dose-dependent sparing driven by hypofractionation and FLASH effect

Guoqiang Zhao[1,‡], Junxiang Wu[1,‡], Da Zhang[1], Jie Li[1], Yi Peng[1], Tiziana Malatesta[2], Lintao Li[1], Shun Lu[1], Jinyi Lang[1], Xianliang Wang[1*], Hao Guo[1*]

Junxiang Wu Co-first author

Corresponding author: Xianliang Wang, Guo Hao

E-mail: wangxianliang@scszlyy.org.cn; guohao@scszlyy.org.cn

Abstract

Purpose: FLASH radiotherapy (FLASH-RT) spares organs at risk (OARs) through the "FLASH effect" and is particularly advantageous under hypofractionation. Breast cancer is theoretically a favorable site for FLASH-RT implementation because the α/β ratio of breast tumors closely approximates that of late-reacting normal tissue. However, the normal-tissue sparing convolves two mechanisms: dose redistribution intrinsic to hypofractionation and the additional biological sparing of the FLASH effect, whose relative contributions across the dose spectrum remain unclear. Because clinical translation of FLASH hinges on the achievable degree of normal-tissue sparing, quantitative modeling grounded in existing experimental evidence is needed. We therefore aimed to disentangle and characterize these two components and assess how they combine in breast cancer.

Methods: Thirty clinically delivered breast VMAT plans (50 Gy/25 fractions) were retrospectively analyzed. Iso-effective hypofractionated regimens (1–5 fractions) preserving tumor biologically effective dose (BED) and relative spatial dose distribution were generated, and a voxel-based FLASH modifying factor (FMF) was applied to simulate the FLASH effect. After converting all regimens to a common conventional-fractionation basis, the sparing of dose-volume histogram (DVH) parameters, normal tissue complication probability (NTCP), and secondary cancer (SC) risk for the lungs, heart,

and contralateral breast was quantified voxel-wise and decomposed into hypofractionation- and FLASH-driven components.

Results: Hypofractionated FLASH regimens consistently reduced OAR dose, NTCP and SC risk, with total sparing increasing as fraction number decreased and reaching largest under single fraction. Hypofractionation dominated low-dose metrics (lung V_5, heart V_5/V_{10}) and long-term SC risk (86-99% of the total Lifetime attributable risk reduction), where FLASH contributed only 1–2%. Conversely, the additional FLASH sparing increased with decreasing fraction number, contributing 11-12% for lung V_{20}, up to 32% for lung V_{30}, and 22% for contralateral breast D_{max}. Under single-fraction delivery, FLASH accounted for 21% and 20% of the NTCP reduction for lungs and heart, respectively. Voxel-wise analysis confirmed spatially complementary mechanisms: hypofractionation spared low-dose regions most, and FLASH sparing was minimal at low doses and increased continuously toward high-dose regions.

Conclusion: In breast cancer, the additional FLASH effect specifically compensates for the limited high-dose-region sparing of hypofractionation, achieving comprehensive OAR protection across the dose spectrum through complementary, dose-dependent mechanisms. These findings support preferentially applying FLASH in ultra-hypofractionated breast RT.

Keywords: FLASH radiotherapy, Breast cancer; Hypofractionation, Late normal-tissue toxicity.

Introduction

Breast cancer is the most common malignancy in women and, when diagnosed at an early stage, carries an excellent prognosis, with a 5-year disease-specific survival rate approaching 98.9% [1]. Adjuvant radiotherapy (RT) is an established component of breast-conserving treatment and postmastectomy management, reducing locoregional recurrence by approximately two-thirds and lowering mortality, one of the most consistent benefits demonstrated in early-stage disease [2-4].

Volumetric-modulated arc therapy (VMAT) achieves highly conformal dose coverage of the breast and regional lymphatic targets through rotational intensity modulation [5]. However, when regional nodal regions such as the internal mammary and supraclavicular nodes are included, the enlarged irradiation volume unavoidably exposes the lungs, heart, and contralateral breast to appreciable dose driven acute and more critical late toxicity, particularly ischemic heart disease and radiation-induced secondary cancers in long-surviving patients [5, 6].

To address these challenges, two new strategies have emerged that are progressively reshaping breast RT. First, Adjuvant radiotherapy is shifting from the conventional 25 fractions toward ultra-hypofractionation (5 or even 1 fraction) [7], and is now progressively moving from preliminary dose exploration toward early clinical implementation. Characterized by a short treatment course, a high single-fraction dose, and precise delivery, this approach shows considerable clinical promise, although its optimal dose and fractionation regimen remain to be determined. This shift has a biological rationale: because the α/β ratio of breast tumors (3–4 Gy) is close to that of late-reacting normal tissue (~3 Gy), the increased late toxicity commonly associated with hypofractionation can potentially be mitigated, making the breast a particularly favorable site for hypofractionation regimens [8, 9]. Second, FLASH-RT, delivered at ultra-high dose rates (>40 Gy/s), spares normal tissue while preserving tumor control, with sparing that becomes increasingly pronounced at higher dose per fraction[10-15]. Preclinical studies have demonstrated significant OAR sparing at equivalent tumor control for hypofractionation regimens (>5 Gy/f) relative to conventional dose rates (<0.04 Gy/s) [10, 13, 14], and the first-in-human application confirmed reduced normal-tissue toxicity with effective tumor control [10]. Crucially, these two strategies converge: because FLASH sparing is most pronounced at hypofractionation regimens, ultra-hypofractionation and FLASH are naturally synergistic. This convergence positions

hypofractionated FLASH as a particularly promising future direction for breast cancer RT.

Based on this rationale, recent treatment-planning studies have begun to explore the potential therapeutic advantage of hypofractionated FLASH-RT. Hörberger et al. introduced the concept of "netsparing", the balance between FLASH-induced normal-tissue sparing and the increased toxicity from larger fraction doses, and demonstrated that tumor sites with small tumor α/β ratios, such as breast and prostate, can achieve positive net sparing [7, 16]. However, because FLASH is suitable to be implemented by hypofractionation, the observed sparing represents a convolution of two distinct mechanisms: the dose-redistribution effect of hypofractionation and the additional biological sparing of the FLASH effect. Prior work [16] has characterized their combined benefit without quantitatively partitioning the contribution of the additional FLASH effect from that of hypofractionation, nor clarifying how the two vary across the dose spectrum and whether they act redundantly or complementarily. This distinction is clinically decisive, as it determines how much of the observed benefit is attributable to FLASH itself rather than to hypofractionation, thereby revealing the true added value of this technology.

To address this issue, we performed a retrospective in-silico treatment-planning and modeling analysis of 30 clinically delivered breast VMAT plans (50 Gy/25 fractions), comparing them with iso-effective hypofractionated (1–5 fractions) and FLASH-modified scenarios. A voxel-based FLASH-modifying factor was used to simulate FLASH sparing under equivalent tumor BED, and all regimens were converted back to a common conventional-fractionation basis to enable direct comparison. We adopted "sparing" as the core metric, defined as the relative difference in a given quantifier between the standard and converted regimens, and evaluated it across multiple dimensions spanning dosimetry (DVH parameters) and radiobiological risk (NTCP and secondary cancer risk). On this basis, we specifically sought to: (1) Systematically quantify the total dosimetric and radiobiological sparing achievable by hypofractionated FLASH under matched dose conformity with conventional VMAT plans, thereby examining the problem at a fundamental level driven solely by fractionation and FLASH-induced sparing. (2) Disentangle this total sparing into its hypofractionation-driven and FLASH-driven components. (3) Reveal their dose-dependent patterns and complementarity through voxel-wise analysis. This framework aims to inform the optimal regimen selection and fractionation

strategy for hypofractionated FLASH-RT in breast cancer.

Materials and Methods

Standard treatment plans

This retrospective study included 30 conventional VMAT plans from 30 breast cancer patients. The plans were used "as is" and were not re-optimized. Patient characteristics and target details are summarized in the Appendix (Table A1). The study was approved by the Institutional Ethics Committee of our hospital (Sichuan Cancer hospital & institution).

Target volumes and organs at risk (OARs, comprising the lungs, heart, and contralateral breast) were delineated using MIM commercial software and transferred to Pinnacle for VMAT planning, prescribed to 50 Gy in 25 fractions [16]. Plans were optimized in the Pinnacle treatment planning system (TPS) to achieve the clinical goal of the prescribed dose covering at least 95% of the target volume while keeping the maximum dose below 110% of the prescribed dose, and to meet the OAR dose constraints recommended by international guidelines and consensus as closely as possible [17].

Alternative fractionated treatments (ALT)

The biologically effective dose (BED) is widely used in clinical practice to compare different fractionation regimens with respect to tumor control and normal tissue toxicity [18]. Based on the linear-quadratic (LQ) model, the *BED* for *n* fractions and a dose per fraction *d* is given by Eq. (1):

$$BED_{\alpha/\beta} = n \times d \left(1 + \frac{d}{\alpha/\beta}\right) \quad (1)$$

where α/β is the α/β ratio of the tumor or normal tissue. The alternative regimens (1–5 fractions), which employ a higher dose per fraction, were generated by scaling the standard dose distribution to an equal tumor BED (Figure 1a, Step 1). Specifically, the dose in each voxel was multiplied by a regimen-specific coefficient derived from the BED formalism, using an α/β of 3.5 Gy for breast tumor [9]. This approach preserves identical relative spatial dose distributions between the standard and alternative regimens. The corresponding dose per fraction for each fractionation scheme is provided in the Appendix (Table A2).

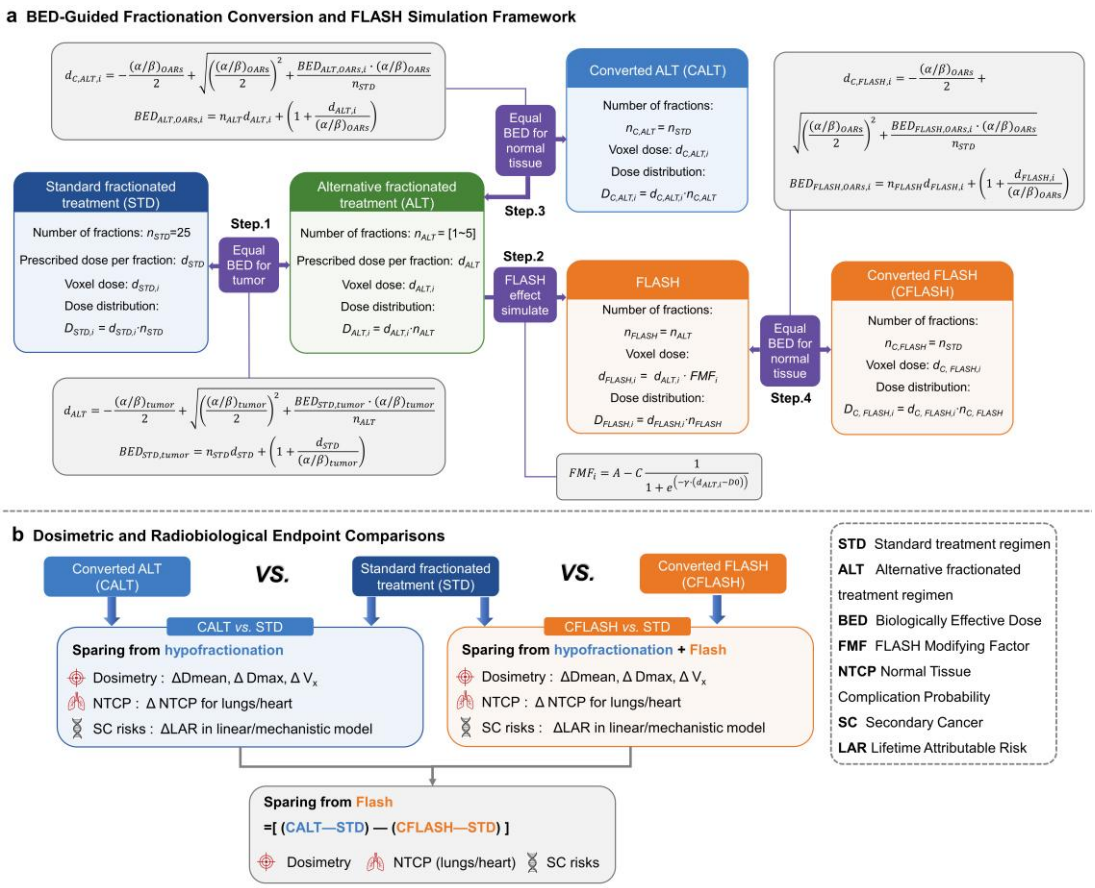


Figure. 1 (a) BED-guided fractionation conversion and FLASH simulation framework. Workflow for generating alternative fractionation (ALT) and FLASH regimens from a standard treatment (STD) using the linear-quadratic (LQ) model and biologically effective dose (BED) constraints. Tumor BED equivalence was used to derive the ALT regimen, whereas FLASH simulation additionally incorporated the FLASH-modifying factor (FMF) to model normal tissue sparing. Converted ALT and FLASH plans were then generated under equal normal tissue BED conditions. Gray boxes indicate the corresponding BED conversion equations. (b) Dosimetric and radiobiological sparing from hypofractionation and FLASH, derived by comparing the converted ALT and converted FLASH regimens with the STD regimen. Endpoints include dose metrics (ΔDmean, ΔDmax, ΔVx), NTCP, and secondary cancer (SC) risk estimated from the lifetime attributable risk (LAR) using linear and mechanistic models.

The simulated FLASH regimens

We assumed that every voxel in the FLASH-RT plan satisfied all conditions required to induce the FLASH effect, including dose rate and irradiation time. In this part, the FLASH and alternative regimens shared the same number of fractions. The FLASH effect was simulated on a voxel-by-voxel basis within the patient anatomy only on normal tissues, not on target. This effect was characterized

as a function of dose and expressed as a dose-modifying factor, the FLASH-modifying factor (FMF), which defines the relative equivalent-dose ratio for each voxel under ultra-high-dose-rate conditions [19, 20]. The FMF is formulated as Eq. (2):

$$FMF(d_i) = A - C\frac{1}{1+e^{\left(-\gamma\cdot(d_i-D0)\right)}} \quad (2)$$

where d_i is the voxel dose, A is the asymptotic maximum and γ, D0 and C are fitting parameters. The FMF was modeled using a logistic function based on preclinical data[16, 20], details as shown in Appendix (Figure A1).

After deriving the FMF, the OAR voxel dose in the FLASH regimen was obtained by multiplying the fractional voxel dose by the FMF, under the assumption that tumor control remained unaffected (Figure 1a, Step 2). The resulting FMF-weighted FLASH simulation regimen thus yields a tumor BED equivalent to that of the standard treatment regimen, while providing a voxel-wise quantification of the FLASH effect in the OARs.

Quantify dosimetric and radiobiological discrepancy

To enable direct comparison of dosimetric and radiobiological endpoints across regimens with different fractionation schedules, the FLASH and alternative regimens were converted back to their equivalent standard fractionated regimens (Figure 1a, Steps 3–4, and Figure 1b). This conversion was performed voxel-by-voxel on the basis of equal normal-tissue BED, using an NT α/β value of 3.0 Gy. The dosimetric and radiobiological sparing effects of the converted alternative fractionated and FMF-weighted FLASH regimens were then evaluated across different fractionation schemes (1–5 fractions).

A. Dosimetric differences

For each fractionation scheme, the normal-tissue sparing effect was defined as the relative difference in clinically relevant DVH parameters (e.g., D_{mean}, V_5, V_{20} et al.) between the standard and converted regimens, expressed as a fraction of the standard-regimen value.

B. NTCP differences

NTCP values for radiation-induced pneumonitis and heart disease were calculated using the Lyman–Kutcher–Burman model for lung (TD50 = 30.80 Gy, n = 0.98, m = 0.37) and the relative-seriality model for heart (TD50 = 52.4 Gy, s = 1.0, γ = 1.3) [21, 22].

C. SC risk differences

Secondary cancer (SC) risk was estimated using Schneider's site-specific carcinoma-induction model, which combines the initial slope of the linear no-threshold (LNT) model with a mechanistic linear-quadratic (LQ) framework accounting for cell killing, tumor induction, and cellular repopulation and repair [23, 24]. Within this framework, the excess absolute risk (EAR) for a given organ is calculated from Eqs. (3)–(5) and depends on: the organ-specific initial slope (β) of the LNT model; a population adjustment term (μ) that incorporates age at exposure (age_x), attained age (age_a), and sex (s); and the organ-equivalent dose (OED), computed voxel-by-voxel and scaled according to the risk-equivalent dose (RED) [25]. Two RED models were implemented in this work. The first is the mechanistic model described above, which accounts for cell death, regeneration, and repair (Eq. 6), where D_T is the prescription dose and d_T is the dose per fraction. The second is a linear model, in which the RED is described by the mean organ dose, giving the overall LNT-based expression for EAR (Eqs. 7–8). The lifetime attributable risk (LAR) [25] was obtained by integrating the EAR between two defined time points, weighted by the baseline survival probability (P) over that interval for a person of the specified age and sex (Eq. 9).

$$EAR(D, agex, agea, s) = \beta_{EAR} OED(D) \mu(agex, agea, s) \quad (3)$$

$$\mu(agex, agea, s) = exp\left(\gamma_e (agex - 30) + \gamma_a \ln(\tfrac{agea}{70})\right) \times (1 \pm 0.17),$$

$$+for females, -for males \quad (4)$$

$$OED = \tfrac{1}{V_T} \textstyle\sum_i V(D_i)\, RED(D_i) \quad (5)$$

$$RED(D) = \tfrac{e^{-\alpha' D}}{\alpha' R}\left(1 - 2R + R^2 e^{\alpha' D} - (1-R)^2 e^{-\frac{\alpha' R}{1-R} D}\right), where\ \alpha' = \alpha + \beta \tfrac{D}{D_T} d_T$$

$$(6)$$

$$RED(D) = D \quad (7)$$

$$EAR(D, agex, agea, s) = \beta_{EAR} \overline{D} \mu(agex, agea, s) \quad (8)$$

$$LAR(D, agex, agea) = \textstyle\int_{agex+L}^{agea} EAR(D, agex, agea) P(agex, agea) da \quad (9)$$

For breast cancer, the FMF-weighted dose distribution derived in this study represents the FLASH-induced modification of normal tissue, expressed as an equivalent conventional fractionation.

This conversion enables a direct radiobiological comparison of the OARs within the PTV between the FMF-weighted FLASH regimen and the standard clinical regimen. All calculations were performed with an in-house Python program, using the widely accepted α/β values of 3.5 Gy for breast tumor [9] and 3.0 Gy for late-reacting normal tissue [20].

Results

Thirty standard fractionated plans (2 Gy × 25 fractions) from 30 patients, together with their corresponding alternative fractionated and FLASH regimens, were analyzed in this study. The dose per fraction for each alternative fractionated regimen (1–5 fractions), derived to preserve equivalent anti-tumor efficacy under the BED formalism, is summarized in Appendix (Table A2).

Dosimetric sparing

Figure 2 shows, for each OAR DVH parameter, the total sparing achieved by the FLASH-converted hypofractionated plans relative to standard fractionation, decomposed into the relative contributions of hypofractionation and of the FLASH effect (the two stacked segments sum to 100% of the total sparing). Total sparing denotes the relative reduction of the parameter, whereas the segment labels denote the percentage of that reduction attributable to each mechanism.

Total sparing increased monotonically as the fraction number decreased for nearly all endpoints, and was largest for the low-dose metrics (V_5) of the contralateral lung and heart, reaching 62% and 68% under single-fraction delivery. Hypofractionation was the dominant mechanism throughout, accounting for at least 68% of the total sparing and being near-complete for low-dose metrics (lung V_5, heart V_5 and V_{10}, and contralateral-breast Dmean), where FLASH contributed only 1–2%. The relative FLASH contribution grew with dose level and decreasing fraction number, rising under single-fraction delivery to 11–12% for lung V_{20}, 22% for contralateral-breast Dmax, and 32% for lung V_{30}. In absolute terms, the OAR DVH parameters under the FLASH regimens were substantially lower than under standard fractionation and decreased progressively with fewer fractions (Appendix Figure A2-A3); for example, lungs V_5 fell from 37% to 23% under single-fraction delivery.

NTCP sparing

Figure 3 shows the NTCP for radiation-induced pneumonitis and cardiac disease, together with the decomposed contributions of hypofractionation and FLASH effect to the total NTCP reduction.

Relative to standard fractionation, the mean NTCP under the FLASH regimen decreased from 1.7% to 1.1% for the lung and from 0.05% to 0.02% for the heart. These confirmed that the absolute risk of both complications is very low in breast cancer patients. Consistent with the dosimetric results, hypofractionation was the dominant mechanism, accounting for ⩾79% of the total NTCP reduction in the lung and ⩾80% in the heart. The relative FLASH contribution rose monotonically as the fraction number decreased, from 10% to 21% for the lung and from 3% to 20% for the heart under single-fraction delivery.

Secondary cancer risk (LAR)

The LAR was used to express the overall magnitude of excess risk above baseline, assessed over a 25-year period [26]. The total, FLASH-additional and hypofractionation-induced sparing of the LAR for the lung and contralateral breast are shown in Figure 4 for both the linear and mechanistic dose–response models. The total sparing increased with decreasing fraction number for both organs, but hypofractionation accounted for 86–99% of the total reduction across all scenarios.

The FLASH contribution was markedly model dependent. Under the linear model, the FLASH-additional sparing of LAR in the lung escalated progressively from 7% to 14% as the fraction number decreased from 5 to 1, consistent with the increasing magnitude of the FLASH effect at higher dose per fraction. However, a totally different trend was observed for the contralateral breast, where the FLASH contribution remains 2%. Under the mechanistic model, however, the FLASH-additional sparing was nearly constant at approximately 1% across all fractionation regimens for both organs, showing no appreciable increase with decreasing fraction number. Both the lungs and the contralateral breast exhibited absolute LAR estimates below 1‰ under both the linear and mechanistic models (Appendix Figure A4), confirming an exceedingly low modeled risk of radiation-induced secondary cancer in patients with breast cancer.

This inter-model discrepancy was organ consistent: both the lung and contralateral breast exhibited the same qualitative pattern of a large linear-model estimate versus a negligible mechanistic-model estimate. Despite these quantitative differences, both models agreed that hypofractionation was the dominant driver of the overall LAR reduction and that the absolute magnitude of FLASH-induced LAR sparing remained modest relative to the hypofractionation component.

Voxel-wise dose-dependent analysis

To elucidate the dose-dependent mechanisms underlying hypofractionation- and FLASH-induced sparing, the voxel-wise dose difference and corresponding sparing were analyzed as a function of the standard-regimen voxel dose $D_{STD,\,i}$ (Figure 5). Hypofractionation redistributed the dose across the OARs: the reduction peaked at intermediate doses (~15–20 Gy), diminished toward higher doses, and became positive above ~43 Gy (Figure 5a); accordingly, the corresponding sparing was largest in low-dose regions (~40–70%) and declined monotonically to zero near 43 Gy (Figure 5c). The FLASH effect showed the opposite dose dependence—negligible at low doses and increasing monotonically with voxel dose (Figure 5b)—with the corresponding sparing rising continuously with both voxel dose and decreasing fraction number, reaching its maximum in high-dose regions under single-fraction delivery (Figure 5d). Thus, hypofractionation and FLASH preferentially act on distinct regions of the dose spectrum.

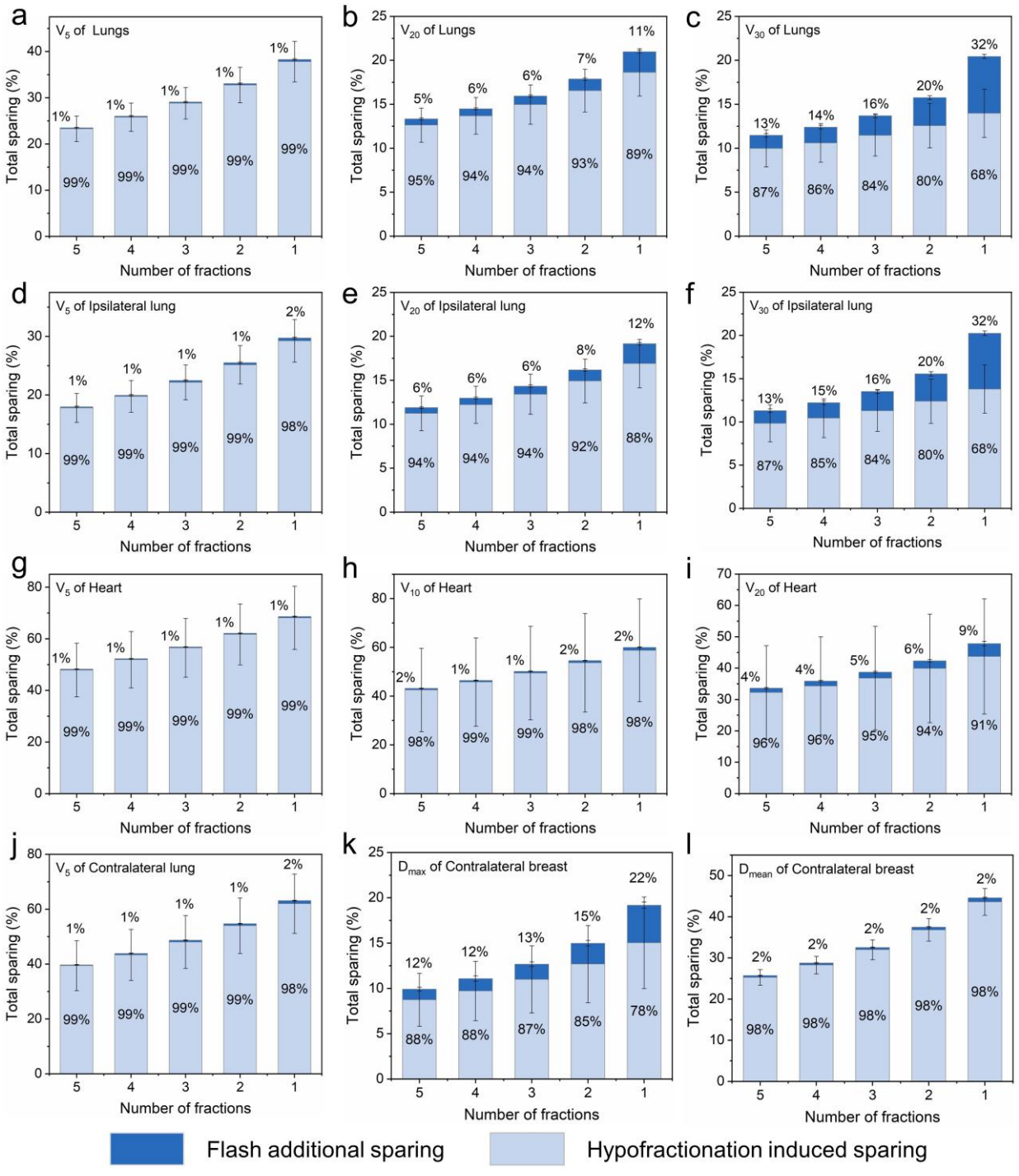


Figure. 2 Total sparing, FLASH additional sparing and hypofractionation induced sparing (%) for various dosimetric parameters of OARs as a function of treatment fractions. (a-c) lungs, (d-f) ipsilateral lung, (g-i) heart, (j) contralateral lung and (k-l) contralateral breast. Total sparing was defined as the change in given OARs DVH-parameters of the converted FLASH treatment relative to that of the standard fractionated treatment. Total sparing represents the combined contribution of the FLASH effect and hypofractionation sparing components.

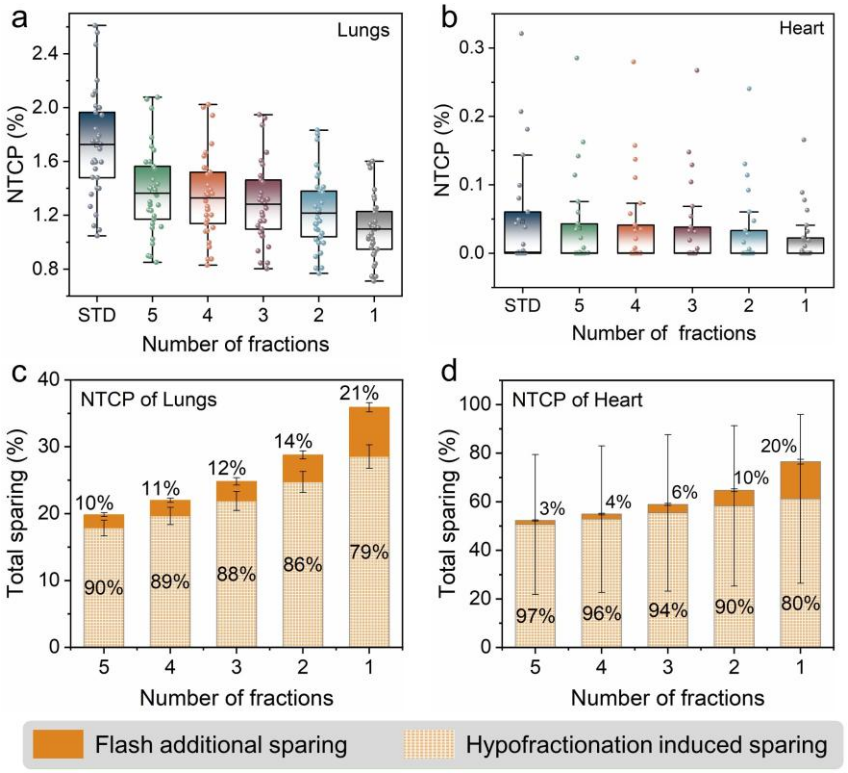


Figure. 3 NTCP of lungs (a), heart (b) and corresponding sparing (c-d) for standard and FLASH regimens as a function of fractions (n_{FLASH}). STD: standard fractionated treatment, 25 fractions.

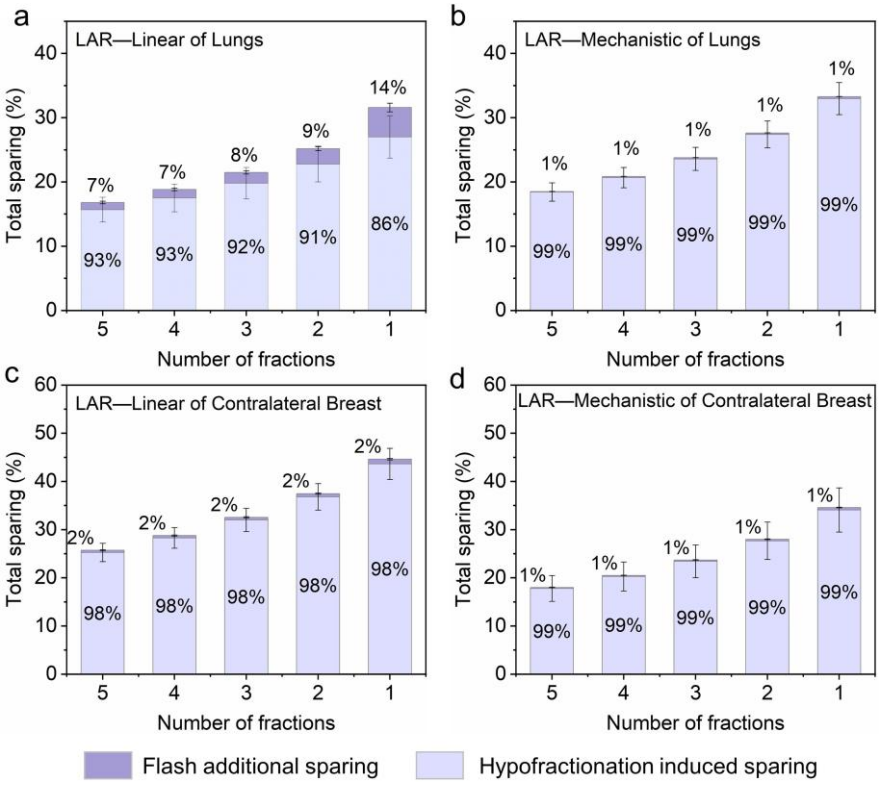


Figure. 4 Total sparing, FLASH additional sparing and hypofractionation induced sparing (%) for LAR (‰) of lungs (a-b) and contralateral breast (c-d) in linear model and mechanistic model as a function of total treatment fractions.

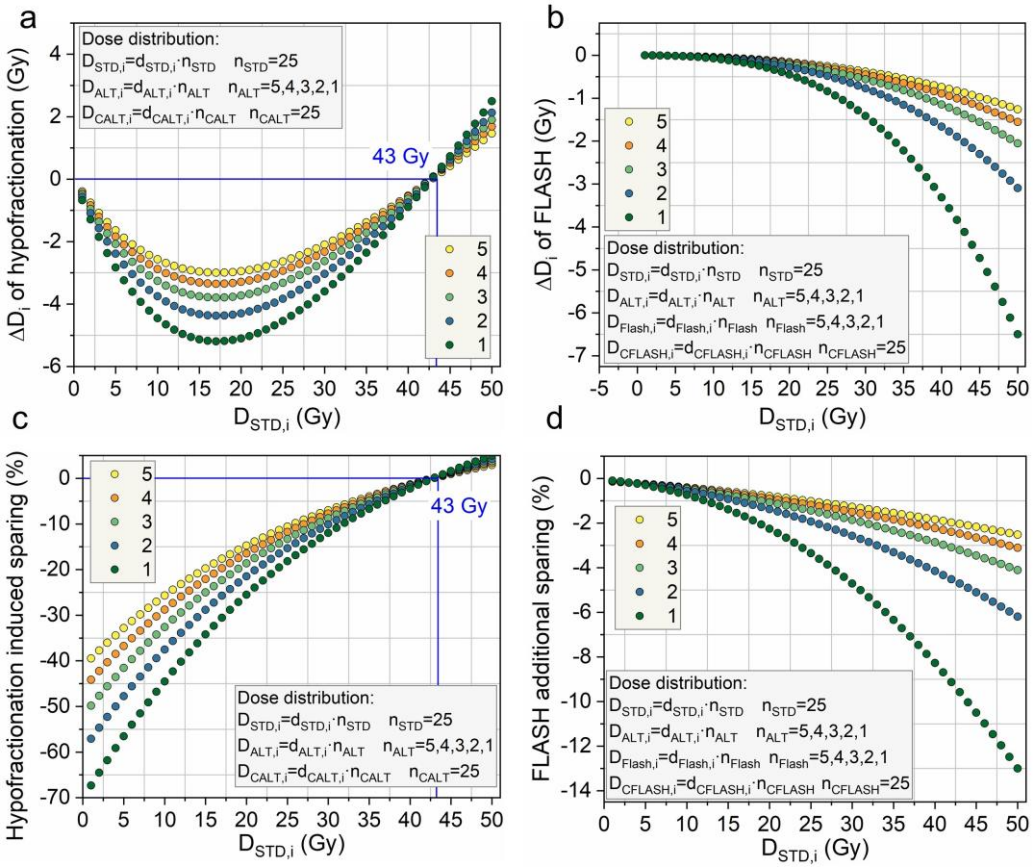


Figure. 5 Voxel dosimetric difference and corresponding sparing as a function of voxel dose. (a-b) Voxel dosimetric difference between hypofractionation as well as FLASH and STD treatment regimens. (c-d) Voxel sparing between hypofractionation as well as FLASH and STD treatment regimens.

Discussion

The successful clinical translation of FLASH radiotherapy critically depends on the degree of normal-tissue sparing that can be achieved, which must be assessed and modeled from existing experimental evidence. In this study, we compared 30 standard breast cancer regimens with corresponding voxel-based hypofractionated FLASH regimens (5–1 fractions) across dosimetric (V_5, V_{20}, etc.) and radiobiological (NTCP and secondary cancer risk) parameters. Our aims were to investigate the potential clinical benefits of FLASH for breast cancer, and to explicitly distinguish the sparing attributable to the additional FLASH effect from that of hypofractionation itself. Under the premise of equivalent tumor control (iso-effective BED), we observed substantial reductions in OAR dose and associated risks across multiple dimensions. Although these reductions were predominantly driven by hypofractionation, the FLASH effect contributed an additional, dose-dependent benefit that

was maximized under ultra-hypofractionated delivery — supporting the translational potential of hypofractionated FLASH radiotherapy in breast cancer [14].

Distinct dose-region contributions of hypofractionation and FLASH effect

Hypofractionation was the principal driver across all organs, contributing at least two-thirds of the total sparing, while FLASH added a smaller and strongly dose-dependent contribution. This reflects where each mechanism acts: hypofractionation lowers integral dose and efficiently spares low- and intermediate-dose regions, explaining its near-complete dominance for low-dose metrics; the FLASH effect is elicited only above dose-rate and dose thresholds and is confined to high-dose regions, so its relative contribution rose from negligible values for V_5 to 32% for lung V_{30}, and further at lower fraction numbers. In absolute terms, single-fraction FLASH reduced heart V_5/V_{10}/V_{20} by up to ~69%, lung V_{20}/V_{30} by ~20–36%, and contralateral-breast Dmax by ~22%. These magnitudes exceed what geometric plan optimization alone can typically achieve, and clinically meaningful given that ischemic heart disease and radiation pneumonitis remain the principal late toxicities in breast RT [27].

Two caveats apply. First, the segment labels in Figure 2 represent proportional attribution rather than absolute reduction. Second, the FLASH contribution depends on the assumed FMF model and thresholds and should be regarded as a model-based estimate. Nonetheless, the overall pattern supports prioritizing ultra-hypofractionated regimens when minimizing deterministic late toxicity is the goal.

Complementary contributions to NTCP reduction

Although the possibility of radiation-induced pneumonitis and cardiac toxicity in breast radiotherapy are relatively low, hypofractionated FLASH regimen achieved substantial comparative reductions (approximately 19.8% ~ 35.9% for lung and 49.2% ~ 74.5% for heart). Because NTCP integrates dose across the whole organ, the near-doubling of the FLASH contribution under single-fraction delivery — reaching 21% for lung and 20% for heart — indicates that the high-dose region becomes a progressively larger determinant of complication risk as fractionation is reduced. This finding is clinically relevant: because further NTCP reduction through geometric optimization alone is limited in modern VMAT plans [28], the additional FLASH contribution identifies ultra-hypofractionated FLASH-RT as a promising route to overcome this optimization plateau, either by lowering residual toxicity or by enabling modest dose escalation. Nonetheless, the absolute NTCP

values should be interpreted with caution, whereas the relative comparisons across regimens are more robust.

Model dependence of FLASH-induced sparing in secondary cancer risk

The divergence between the linear and mechanistic models (Figure 4) stems from different assumptions about the dose–response for carcinogenesis at high doses. Under the linear model, each unit of dose reduction lowers risk proportionally, so FLASH sparing concentrated in high-dose voxels is maximally credited, and the rise from 7% to 14% in the lung tracks the larger FMF reductions at lower fraction numbers. Meanwhile, as shown in Eq. (7), the LAR estimated using the linear model exhibited a linear relationship with the mean dose. Accordingly, the relative contributions of hypofractionation- and FLASH-induced sparing in the contralateral breast followed a trend consistent with changes in its Dmean (Figure 2l). The mechanistic model incorporates cell killing and repopulation; for lung ($R = 0.83$, $\alpha = 0.042\ Gy^{-1}$), the RED curve plateaus at high doses as lethal killing removes cells from the at-risk pool. FLASH-induced reductions in high-dose voxels therefore change RED, OED, and LAR only marginally, explaining both the small (~1%) and near-constant mechanistic FLASH contribution. This behavior is consistent with Johnson et al [29], who reported similar linear–mechanistic divergence within the Schneider framework. The two models thus bracket the plausible range of FLASH-induced LAR sparing as upper and lower bounds, respectively.

Importantly, this ambiguity applies only to the stochastic carcinogenesis endpoint, not to the NTCP results, which reflect deterministic late toxicity. The FLASH contributions to NTCP reduction are therefore a more robust estimate of the incremental FLASH benefit. Taken together, the simultaneous reduction of NTCP and LAR indicates a dual clinical benefit — reduced deterministic late toxicity and probable, though model-dependent, decrease in long-term SC risks — particularly valuable in breast cancer given long survival and low-dose-bath concerns in the contralateral breast [25, 29].

Voxel-wise mechanistic basis

The voxel-wise analysis (Figure 5) clarifies the mechanistic basis of the organ-level behavior. Hypofractionation exploits the tumor–normal-tissue α/β difference to preferentially spare low- and intermediate-dose voxels. However, it offers no benefit and even increases the biological dose in the

highest-dose voxels near the target, consistent with the crossover above ~43 Gy. The FLASH effect follows the opposite dose dependence, active only above voxel-dose and dose-rate thresholds and reinforced at larger doses per fraction. This dose-partitioned view explains why the two mechanisms exhibit a complementary relationship: the former preferentially reduces the biological burden across the low- and intermediate-dose regions, whereas the latter provides additional protection in high-dose regions where radiation-induced toxicity is most likely to occur. This complementary relationship implies diminishing returns for adding FLASH to highly fractionated schedules, alongside the largest incremental benefit under ultra-hypofractionated delivery.

Limitations

A fundamental limitation stems from the nature of this work. No consensus model yet links delivery parameters (dose rate, single-fraction dose, etc.) to the magnitude of normal-tissue sparing in an organ-specific manner. The simplified FMF parameterization used here is derived from pooled preclinical data, leaving uncertainty in its parameters (A, γ, D_0) and their transferability to human tissues. These data are moreover largely based on single-fraction irradiations of small volumes across heterogeneous biological systems and endpoints, so their applicability to multi-fractionated ultra-high-dose-rate delivery is not yet established. The present study should therefore be regarded as a mechanistic in-silico analysis rather than a predictive clinical tool. The absolute values reported here carry uncertainty, whereas the more robust findings are the comparative and dose-partitioned trends, which are largely preserved irrespective of the parameters assumed. Prospective validation incorporating measured dose-rate distributions and clinically observed toxicity endpoints will be essential before these results can inform treatment decisions.

Several additional limitations apply. First, the analysis assumes that all target voxels satisfy the dose-rate and irradiation-time criteria required to trigger the FLASH effect, which may not hold in practice, particularly for deep-seated targets or VMAT delivery; the reported FLASH contributions therefore represent an upper estimate of the achievable in vivo benefit.

Second, our BED-based fractionation conversion relies on the linear-quadratic (LQ) formalism, whose validity at large doses per fraction (>10 Gy) remains debated; alternatives such as the linear-quadratic-linear (LQ-L) model have been proposed to better describe the high-dose response. This is

relevant to our single- and ultra-hypofractionated regimens, where the prescribed fraction dose can exceed 10 Gy. However, this is unlikely to weaken our conclusion. Böhlen et al. found that a smaller FLASH effect was required to offset the increased late toxicity predicted at higher fraction doses under the LQ-L model [20], implying that the net high-dose sparing for small fraction numbers could be even more favorable than the LQ-based estimate — consistent with our finding that the additional FLASH benefit is concentrated in high-dose regions under ultra-hypofractionation. Moreover, because organs at risk receive far lower fraction doses than the prescription owing to geometric sparing, the LQ model remains applicable in most voxels even at higher prescribed fraction doses. Nonetheless, the LQ-L model itself relies on parameters that are not extensively validated [20], and the influence of the high-dose response model warrants dedicated investigation.

Third, the mechanistic carcinogenesis parameters (R, α) are derived from Hodgkin lymphoma survivor data [23] and may not transfer directly to breast cancer, and neither carcinogenesis model accounts for a possible difference in relative biological effectiveness for oncogenic transformation between FLASH and conventional dose rates. Finally, the 25-year LAR window may underestimate the lifetime risk in young patients.

Despite these caveats, the convergence of both dose–response models on hypofractionation as the dominant driver of LAR reduction (86–99%), together with the model-independent NTCP benefit, provides a robust lower bound for the clinical benefit achievable with hypofractionated FLASH breast radiotherapy.

Conclusion

Using a voxel-based, BED-guided modelling framework, this study systematically quantified the dosimetric and radiobiological sparing achievable with hypofractionated FLASH-RT in breast cancer and, for the first time, partitioned it into its hypofractionation- and FLASH effect -driven components. Under equivalent tumor control, comparing with conventional fractionated regimens, hypofractionated FLASH regimens consistently reduced OAR doses, NTCP, and SC risks, with hypofractionation accounting for the majority of the observed reductions, and the greatest overall benefit observed for single-fraction regimens. Importantly, this work distinguished the respective contributions of hypofractionation and the additional FLASH effect, demonstrating complementary dose-dependent

sparing mechanisms: hypofractionation predominantly reduced the biological burden in low- and intermediate-dose regions, whereas the additional FLASH effect preferentially enhanced sparing in high-dose regions. These findings provide a quantitative framework for evaluating the therapeutic benefits of FLASH-RT in breast cancer and indicate that its clinical benefit is maximised when combined with ultra-hypofractionated regimens.

Acknowledgements

None.

Author contributions

Study concept and design of the Research: GQZ, JXW, DZ, SL, JYL; Acquisition of data and images dataset processing: GQZ, JXW, XLW, YP, HG; Analysis and interpretation of data: GQZ, JL, LTL, JXW, YP, HG; Manuscript Preparation: GQZ, XLW, HG, JL; Writing Manuscript GQZ, XLW, HG; Manuscript critical revision: GQZ, JXW, LTL, JL, XLW, HG; All authors read and approved the final manuscript.

Funding

Sichuan Cancer Hospital Outstanding Youth Fund, China, YB2025014.

Young Scientists Fund of the Natural Science Foundation of China, No.12505391

Noncommunicable Chronic Diseases-National Science and Technology Major Project, China, 2024ZD0519900, 2024ZD0519901

Sichuan Provincial Natural Science Foundation of China, 2026NSFSC0734

Data availability

No datasets were generated or analysed during the current study.

Declarations

Ethics approval and consent to participate

The authors declare that this retrospective study “Dosimetric and radiobiological benefits of FLASH radiotherapy in breast cancer: complementary dose-dependent sparing driven by hypofractionation and the FLASH effect” received the approval of the ethic committee of Sichuan Cancer Hospital located in 55th Renmin South Road, 4th Section, 610041, Chengdu, China. This study was conducted in

accordance with the Declaration of Helsinki.

Consent for publication

Even if no individual patient data were reported, consensus has been received by every patient for the elaboration of its data and for future scientific publication.

Competing interests

The authors declare no competing interests.

Author details

[1]Department of Radiation Oncology, Precision Radiation in Oncology Key Laboratory of Sichuan Province, Sichuan Clinical Research Center for Cancer, Sichuan Cancer Hospital & Institute, Sichuan Cancer Center, Affiliated Cancer Hospital of University of Electronic Science and Technology of China, Chengdu, China

[2]Department of Radiotherapy and Medical Oncology and Radiology, Isola Tiberina – Gemelli Isola Hospital, Rome, Italy

References

1. Hoekstra N, Fleury E, Merino Lara TR, van der Baan P, Bahnerth A, Struik G, et al. Long-term risks of secondary cancer for various whole and partial breast irradiation techniques. Radiother Oncol. 2018; 128(3): 428-33.
2. Ragaz J, Jackson SM, Le N, Plenderleith IH, Spinelli JJ, Basco VE, et al. Adjuvant radiotherapy and chemotherapy in node-positive premenopausal women with breast cancer. N Engl J Med. 1997; 337(14): 956-62.
3. Feigenberg SJ, Price Mendenhall N, Benda RK, Morris CG. Postmastectomy radiotherapy: patterns of recurrence and long-term disease control using electrons. International Journal of Radiation Oncology*Biology*Physics. 2003; 56(3): 716-25.
4. GROUP EBCT. Effects of radiotherapy and surgery in early breast cancer-an overview of the randomized trials. N Engl J Med. 1995; 333(22): 1444-56.
5. Zhang Y, Huang Y, Ding S, Yuan X, Shu Y, Liang J, et al. A dosimetric and radiobiological evaluation of VMAT following mastectomy for patients with left-sided breast cancer. Radiat Oncol. 2021; 16(1): 171.
6. Darby SC, Ewertz M, McGale P, Bennet AM, Blom-Goldman U, Brønnum D, et al. Risk of ischemic heart disease in women after radiotherapy for breast cancer. N Engl J Med. 2013; 368(11): 987-98.
7. Yarnold JR, Brunt AM, Chatterjee S, Somaiah N, Kirby AM. From 25 fractions to five: how hypofractionation has revolutionised adjuvant breast radiotherapy. Clin Oncol (R Coll Radiol). 2022; 34(5): 332-9.
8. Eric J. Hall AJG. Radiobiology for the radiologist. Australas Phys Eng Sci Med. 2019; 41(4): 1129-30.
9. Qi XS, White J, Li XA. Is α/β for breast cancer really low? Radiother Oncol. 2011; 100(2): 282-8.
10. Bourhis J, Sozzi WJ, Jorge PG, Gaide O, Bailat C, Duclos F, et al. Treatment of a first patient with FLASH-radiotherapy. Radiother Oncol. 2019; 139: 18-22.
11. Suo M, Shen H, Lyu M, Jiang Y, Liao X, Tang W, et al. Biomimetic nano-cancer stem cell scavenger for inhibition of breast cancer recurrence and metastasis after FLASH-radiotherapy. Small. 2024; 20(29): 2400666.
12. Van Marlen P, van de Water S, Dahele M, Slotman BJ, Verbakel WFAR. Single ultra-high dose rate proton transmission beam for whole breast FLASH-irradiation: quantification of FLASH-dose and relation with beam parameters. Cancers (Basel). 2023; 15(9): 2579.
13. Vozenin M, Montay-Gruel P, Tsoutsou P, Limoli CL. Mechanisms, challenges and opportunities for FLASH radiotherapy in cancer. Nat Rev Cancer. 2026; 26(1): 62-75.
14. Melemenidis S, Viswanathan V, Dutt S, Kapadia N, Lau B, Soto LA, et al. Effectiveness of FLASH *vs.* Conventional dose rate radiotherapy in a model of orthotopic, murine breast cancer. Cancers (Basel). 2025; 17(7): 1095.
15. Ghita-Pettigrew M, Brown KH, Kerr BN, Walls GM, Verginadis II, Adrian G, et al. Photon FLASH spares radiation-induced changes in cardiac function, remodelling and arrythmia in a preclinical model. Radiother Oncol. 2026; 216: 111369.
16. Hörberger F, Petersson K, Ceberg S, Bäck S, Adrian G, Ceberg C. Investigating the therapeutic potential of FLASH radiotherapy-a treatment planning study. Radiother Oncol. 2025; 209: 110947.
17. Benedict SH, Yenice KM, Followill D, Galvin JM, Hinson W, Kavanagh B, et al. Stereotactic body radiation therapy: the report of AAPM task group 101. Med Phys. 2010; 37(8): 4078-101.
18. Jones B, Dale RG, Deehan C, Hopkins KI, Morgan DAL. The role of biologically effective dose (bed) in clinical oncology. Clin Oncol (R Coll Radiol). 2001; 13(2): 71-81.
19. Böhlen TT, Germond J, Bourhis J, Bailat C, Bochud F, Moeckli R. The minimal FLASH sparing effect needed to compensate the increase of radiobiological damage due to hypofractionation for late-reacting tissues. Med Phys. 2022; 49(12): 7672-82.

20. Böhlen TT, Germond J, Bourhis J, Vozenin M, Ozsahin EM, Bochud F, et al. Normal tissue sparing by FLASH as a function of single-fraction dose: a quantitative analysis. International journal of radiation oncology, biology, physics. 2022; 114(5): 1032-44.
21. Seppenwoolde Y, Lebesque JV, de Jaeger K, Belderbos JSA, Boersma LJ, Schilstra C, et al. Comparing different NTCP models that predict the incidence of radiation pneumonitis. International Journal of Radiation Oncology*Biology*Physics. 2003; 55(3): 724-35.
22. Gagliardi G, Lax I, Ottolenghi A, Rutqvist LE. Long-term cardiac mortality after radiotherapy of breast cancer-application of the relative seriality model. The British Journal of Radiology. 1996; 69(825): 839-46.
23. Schneider U, Sumila M, Robotka J. Site-specific dose-response relationships for cancer induction from the combined japanese a-bomb and hodgkin cohorts for doses relevant to radiotherapy. Theoretical Biology and Medical Modelling. 2011; 8(1): 27.
24. Schneider U. Mechanistic model of radiation-induced cancer after fractionated radiotherapy using the linear-quadratic formula. Med Phys. 2009; 36(4): 1138-43.
25. Johnson PB, Mamalui M, Brodin P, Janssens G. Secondary cancer risk in six anatomical sites when using pat, IMPT, and VMAT/IMRT radiotherapy. Radiother Oncol. 2024; 199: 110421.
26. Smith-Bindman R. Radiation dose associated with common computed tomography examinations and the associated lifetime attributable risk of cancer. Archives of Internal Medicine. 2009; (22): 2078.
27. Banfill K, Giuliani M, Aznar M, Franks K, McWilliam A, Schmitt M, et al. Cardiac toxicity of thoracic radiotherapy: existing evidence and future directions. J Thorac Oncol. 2021; 16(2): 216-27.
28. Yorke E. Modeling clinical outcomes in radiotherapy: NTCP, TCP and the “tecs”. Med Phys. 2023; 50(S1): 122-4.
29. Otsuka K, Iwasaki T. Insights into radiation carcinogenesis based on dose-rate effects in tissue stem cells. International Journal of Radiation Oncology*Biology*Physics. 2023; 99(10): 1503-21.

Supplementary Files

This is a list of supplementary files associated with this preprint. Click to download.

- Appendix.docx